

33. ORGANIC GEOCHEMISTRY OF ODP LEG 107 SEDIMENTS (SITES 652, 653, 654, 655)¹

E. Brosse² and J. P. Herbin²

ABSTRACT

The Rock-Eval pyrolysis of rock samples and the elemental analysis of kerogens show clear differences between Messinian black shales and Pliocene-Pleistocene sapropels recovered during ODP Leg 107. The Messinian black shales are characterized by a large variety of compositions which probably reflects a great diversity of depositional and diagenetic paleoenvironments. In contrast, the Pliocene-Pleistocene sapropels, occurring as discrete layers in nannofossil oozes barren of organic carbon, constitute a rather homogeneous group in terms of organic content. A considerable contribution of terrestrial organic matter in the sapropels could mean that an identical phenomenon of terrestrial input has been periodically reproduced in the basin. The maturity and the nature of the organic matter are discussed with respect to anomalous values recorded for T_{max} parameter.

INTRODUCTION

The cores from Sites 652, 653, 654, and 655 of ODP Leg 107 give a new opportunity to study, in the Tyrrhenian Sea, two types of organic-rich sediments already known in the periadriatic realm and in more oriental parts of the Mediterranean Sea (Drooger, 1973; Carloni et al., 1974; Borsetti et al., 1975; Deroo et al., 1978; Kidd et al., 1978; Cita, 1982).

1. Black shales of Messinian age, in general finely laminated, that occur as subunits of few meters in thickness, in sediments of evaporitic affinities;

2. Sapropels of uppermost Pliocene and Pleistocene age that occur as discrete layers of few centimeters in thickness within more or less marly nannofossil oozes.

The main contribution of the present work consists in the characterization of kerogens, i.e., of the organic residues obtained after chloroform extraction of solvent-soluble organic matter and dissolution of the mineral matrix.

SAMPLES

Thirty-one samples have been chosen on board ship, for our analyses, based on organic geochemistry data obtained during Leg 107. Seven samples are representative of the Pliocene-Pleistocene sapropels and 23 samples of the Messinian black shales. One sample (107-652A-7R-3, 133–135 cm) is a calcareous ooze which is typical for the host rock surrounding the sapropels (Fig. 1).

The Messinian Black Shales

From Hole 652A, three samples (107-652A-20R-6, 73–74 cm, from lithologic Unit IV, and 107-652A-37R-5, 111–112 cm, and 107-652A-38R-3, 65–67 cm, from Unit V) have been taken in sequences of gypsum and carbonate-bearing sandy silts or sands, with interlayered calcareous clays or muds, which present a turbiditic character. The others (107-652A-62R-1, 125–127 cm; 107-652A-62R-CC, 2–3 cm; 107-652A-63R-3, 81–82 cm; 107-652A-63R-CC, 18–19 cm; 107-652A-64R-1, 104–105 cm; and 107-652A-64R-2, 62–63 cm) belong to a particular subunit (in Unit V) characterized by thinly laminated brown/black clays, especially

rich in organic carbon (up to 11.4% from on-board analyses). The CaCO_3 content is highly variable, averaging ~25%.

The three Messinian samples from Hole 653B (107-653B-25X-1, 129–131; 107-653B-28X-2, 1–3 cm; and 107-653B-28X-2, 88–90 cm) belong to Unit II, composed of various types of sands, silts, and muds interpreted as deposits of restricted marine to evaporitic environments. The CaCO_3 content is low (0%–20%).

Among the 11 Messinian samples of Hole 654A, one (107-654A-28R-2, 35–37 cm) comes from Unit II, of gypsum interbedded with calcareous clay, mudstone, minor sandstone, breccia, dolostone, anhydrite, and very rare nannofossil chalk.

The others (107-654A-36R-2, 41–42 cm; 107-654A-37-CC; 107-654A-38R-1, 17–20 cm; 107-654A-38R-1, 126–130 cm; 107-654A-38R-1, 130–132 cm; 107-654A-38R-2, 44–46 cm; 107-654A-38R-CC; 107-654A-39R-1, 143–145 cm; 107-654A-39R-2, 12–14 cm; and 107-654A-39R-2, 72–73 cm) belong to Unit III, a dark colored, finely laminated, organic carbon-rich claystone and dolomitic to calcareous siltstone, with minor volcanic ash. Radiolaria, sponge spicules, diatoms, and fish teeth are common. In this unit of about 35 m in thickness, the maximum enrichment in organic matter is observed between 338.6 m and 341.7 m, in a layer which presents a very black coloration and a mixed sequence of thin laminations and debris-flow structures. In Section 5 of Core 107-654A-40R, asphaltic matter was observed. The material is believed to have been degraded oil, and contains abundant high-molecular weight hydrocarbon compounds ($> C_{36}$). As a whole, the CaCO_3 content is lower than in the Pliocene-Pleistocene sediments, but it may reach 60%.

The Pliocene-Pleistocene Sapropels

Two samples (107-652A-7R-4, 27–29 cm, and 107-652A-9R-2, 93–95 cm) come from Unit II of Hole 652A, a unit of marly nannofossil ooze: they were taken from the fifth (ST5) and the last (ST8) sapropels encountered in the present hole.

One sample (107-653B-8H-3, 99–101 cm) comes from Subunit Ia of Hole 653B, a grey-brown nannofossil ooze with more or less foraminifers and minor mud. Clastic or cineritic layers are common, and sapropelic layers apparently are more diffuse in the sediment than in Hole 652A.

One sample (107-654A-6R-4, 137–139 cm) comes from Unit I of Hole 654A, very similar to the deposit described above for Unit I of Hole 653B.

Three samples (107-655A-2H-4, 65–66 cm; 107-655A-3H-1, 139–147 cm; 107-655A-3H-4, 69–71 cm) come from the Pliocene-Pleistocene drilled just above the basement in Hole 655A.

¹ Kastens, K. A., Mascle, J., et al., 1990. *Sci. Results, Proc. ODP*, 107: College Station, TX (Ocean Drilling Program).

² Synthèse Géologique et Géochemie, Institut Français du Pétrole, P.B. 311, 92506 Rueil-Malmaison, France.

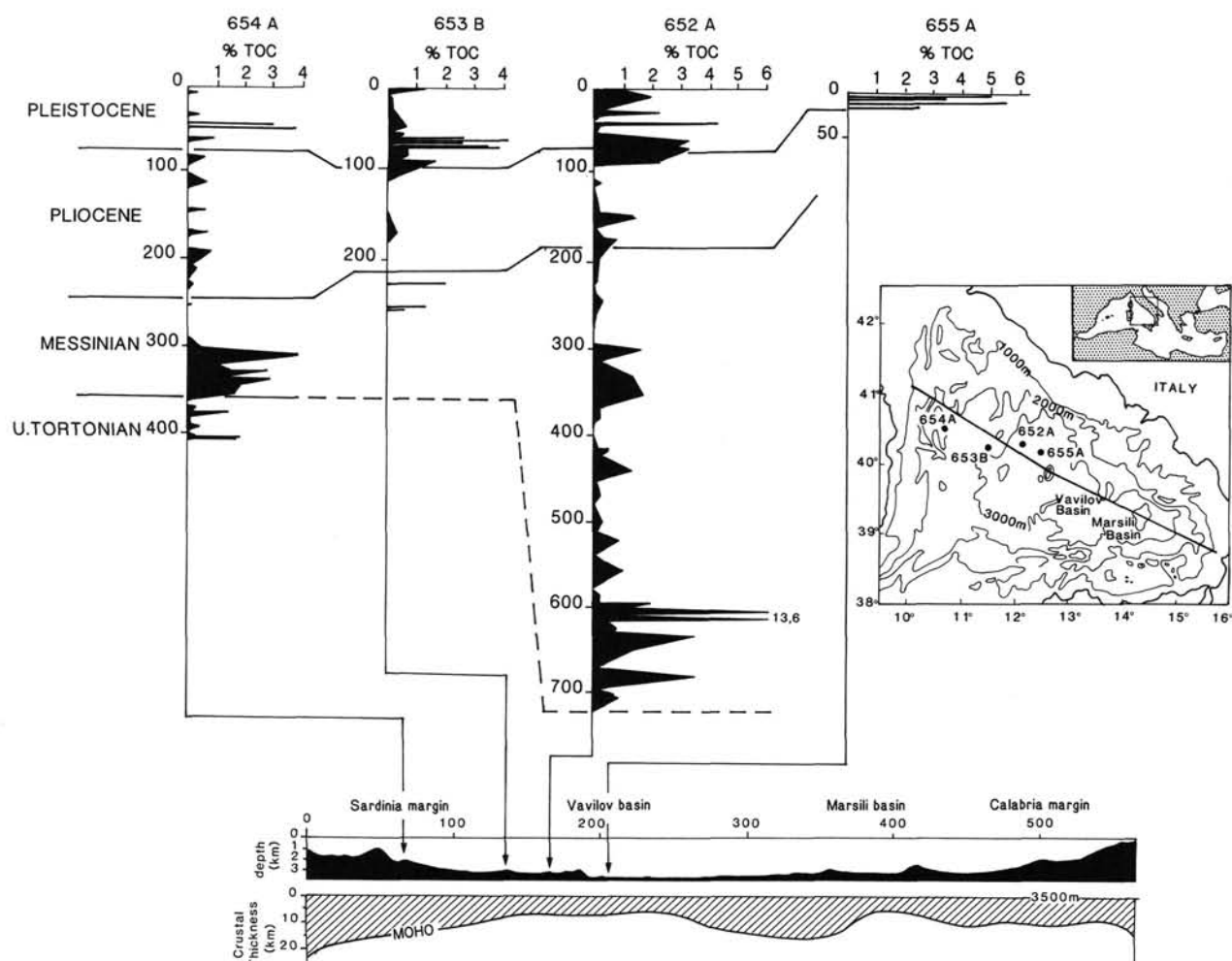


Figure 1. Location of the wells and TOC logs. The location of the four studied wells is given, together with vertical logs of the Total Organic Carbon values, obtained both from our sampling and from shipboard measurements.

This unit is composed of marly nannofossil ooze with occasional volcanoclastic layers and detrital sand layers. Six well-differentiated sapropels or sapropelic layers were recognized. Among our three samples, the first one is black, the second one is olive-grey, and the last one is dark olive-grey.

All the formations from which the samples were taken possess a rather uniform CaCO_3 content of about 50%, except in Hole 653B.

ANALYTICAL METHODS

The 31 whole rock samples (R) were crushed for a Rock-Eval pyrolysis (Table 1) which basically gives (Espitalie et al., 1984, 1985, 1986):

1. Total Organic Carbon (TOC, in weight%) obtained from combustion of the sample at 600°C in the presence of oxygen and detection as CO_2 (Fig. 1);
2. The quantity of free hydrocarbons released by vaporization at 300°C during 3 min (S_1 in mg of HC/g of rock) (HC = hydrocarbons), measured with a Flame Ionization Detector;
3. The quantity of hydrocarbons released during cracking of organic matter between 300°C and 600°C at a heating rate of $25^\circ\text{C}/\text{min}$ (S_2 in mg of HC/g of rock);
4. The temperature corresponding to the maximum flow of hydrocarbons released by cracking (T_{max} in $^\circ\text{C}$);

5. The quantity of CO_2 released from organic matter during the first part of cracking, before the decomposition of carbonates (S_3 in mg of CO_2/g of rock).

$S_1 + S_2$ is a parameter which serves usually to quantify the petroleum potential of a rock. Hydrogen Index (HI, or S_2/TOC) and Oxygen Index (OI, or S_3/TOC) are used to characterize the chemical composition of the organic matter; in the absence of mineral matrix, for instance in coals, the distribution of the values in a HI-OI diagram is very similar to the distribution obtained in the classical (H/C, O/C) Van Krevelen diagram. T_{max} is a rank parameter, i.e., it serves to determine the degree of maturation reached by the rock.

The mineral carbon content of the 31 samples (Table 1) has been measured, by complete dissolution in HCl of the carbonates contained in the crushed rock, and titration with NaOH.

Thirteen samples were chosen for kerogen preparation, because they were representative of the different units, and because they presented sufficiently high TOC values. Firstly they were extracted with chloroform (RAE = rock after extraction), then the solid residue was treated by HCl and HF for complete dissolution of the mineral matrix. Finally, the crude kerogen (KB) obtained was extracted again with chloroform, to give an "extracted chloroform KC" which is really the solid organic matter contained in the rock (Durand and Nicaise, 1980). Rock-Eval pyrolysis has been performed on the extracted rocks and on each type of kerogen (Table 1). And the elemental composition (C, H, O, N, S, Fe) of the KC has been measured (Durand and Monin, 1980) (Table 2).

Table 1. Rock-Eval data for rocks and kerogens. See text for explanation of abbreviations.

Core, section, interval (cm)	Depth (mbsf)	NAT	%CaCO ₃	TOC (%)	S ₁ + S ₂	HI	OI	T _{MAX}
107-652A-								
7R-3, 133-135	69.23	R	23	0.08	0.1			
7R-4, 27-29	69.67	R	38	1.14	1.6	132	232	420
		RAE		3.29	9.5	265	70	425
		KB		45.37	227.5	467	91	417
		KC		44.70	207.3	439	85	417
9R-2, 93-95	86.63	R	33	2.19	5.7	247	186	422
		RAE		2.69	7.7	263	143	422
		KB		43.47	193.4	417	99	415
		KC		39.90	184.3	437	105	415
20R-6, 73-74	198.03	R	6	0.09	0.8			
37R-5, 111-112	361.11	R	28	1.06	0.3	19	144	415
		RAE		0.51	0.1	12	175	421
		KB		11.55	11.1	84	103	422
		KC		19.13	14.7	66	75	426
38R-3, 65-67	367.35	R	8	0.05	1.0			
62R-1, 125-127	596.15	R	30	0.44	0.2	32	232	420
62R-CC, 2-3	603.92	R	24	0.62	0.2	26	153	426
63R-3, 81-82	608.31	R	22	0.56	0.2	36	134	425
63R-CC, 18-19	613.68	R	11	6.06	40.3	621	7	435
		RAE		4.57	23.6	514	7	438
		KB		43.50	270.7	617	11	441
		KC		42.00	276.8	656	8	443
64R-1, 104-105	615.24	R	11	13.65	129.1	890	6	437
		RAE		11.56	89.0	767	6	442
		KB		52.15	434.4	828	5	448
		KC		52.35	452.5	861	4	445
65R-2, 62-63	626.62	R	41	1.03	0.3	31	110	426
107-653B-								
8R-3, 99-101	68.89	R	42	3.88	12.9	318	146	422
		RAE		1.91	5.8	274	175	423
		KB		46.93	185.4	361	83	417
		KC		51.70	177.4	322	79	417
25X-1, 129-131	226.99	R	33	1.99	3.4	162	331	431
		RAE		2.07	2.6	118	235	433
		KB		19.05	84.9	429	59	421
		KC		20.00	84.5	414	65	423
28X-2, 1-3	256.11	R	16	1.24	5.9	456	120	416
		RAE		1.70	5.4	298	71	422
		KB		33.40	169.5	476	49	417
		KC		40.75	207.7	484	42	416
28X-2, 88-90	256.98	R	9	0.52	1.1	198	173	420
107-654A-								
6R-4, 137-139	46.17	R	35	3.84	10.3	248	171	413
		RAE		4.73	10.4	182	124	408
		KB		21.25	63.3	270	98	408
		KC		19.85	60.5	277	97	409
28R-2, 35-37	253.85	R	9	0.03	0.1			
36R-2, 41-42	311.91	R	47	3.72	6.2	127	53	362
		RAE		3.20	5.1	89	51	370
		KB		5.65	33.0	389	72	360
		KC		5.30	24.3	318	55	364
37-CC	328.60	R	20	1.36	4.1	218	96	354
38R-1, 17-20	329.47	R	11	0.89	6.2	575	233	402
38R-1, 126-130	330.50	R	28	1.65	3.1	142	167	379
38R-1, 130-132	330.60	R	10	3.68	17.2	379	82	385
		RAE		2.42	4.1	101	101	370
		KB		19.70	62.7	234	55	383
		KC		20.78	83.5	287	55	380
38R-2, 44-46	331.24	R	8	2.67	20.8	698	66	407
		RAE		1.87	11.5	451	83	391
		KB		16.25	87.4	461	50	392
		KC		20.35	122.8	516	43	392
38R-CC	338.30	R	25	0.83	0.6	66	246	399
39R-1, 143-145	340.03	R	13	1.63	7.7	418	90	398
		RAE		1.77	7.7	342	77	394
39R-2, 12-14	340.22	R	31	2.54	4.9	176	87	395
39R-2, 72-73	340.82	R	14	2.33	5.6	215	97	398
107-655A-								
2H-4, 65-66	5.15	R	19	4.99	15.9	300	141	421
		RAE		5.16	12.9	222	121	425
		KB		45.70	169.2	333	81	413
3H-1, 139-147	14.09	R	33	0.15	0.1	13		
3H-4, 69-71	17.89	R	20	2.35	5.9	236	202	422
		RAE		0.96	1.6	143	363	419
		KB		2.59	5.2	173	119	424
		KC		2.53	5.8	201	118	421

Table 2. Elemental analysis of kerogens KC. See text for discussion.

Core, section, interval (cm)	Depth (mbsf)	C	H	N	O	S	Fe	ASH.	H/C	O/C × 100	N/C	S/C
107-652A-												
7R-4, 27-29	69.67	50.82	5.09	2.38	16.15	11.52	9.10	15.90	1.20	23.83	3.98	0.82
9R-2, 93-95	86.63	47.70	4.53	2.36	15.89	13.01	11.51	20.00	1.14	24.98	4.21	0.00
37R-5, 111-112	361.11	22.75	1.58	0.67	10.74	29.87	25.59	43.70	0.83	35.41	2.50	1.02
63R-CC, 18-19	613.68	42.21	4.78	0.70	3.84	25.39	18.39	30.40	1.36	6.82	1.41	3.83
64R-1, 104-105	615.24	62.46	7.54	1.14	3.86	13.23	9.96	16.40	1.45	4.63	1.55	1.09
107-653B-												
8H-3, 99-101	68.89	50.95	5.11	2.21	18.33	10.16	8.39	19.60	1.20	26.98	3.69	0.41
25X-1, 129-131	226.99	23.71	2.37	0.85	8.20	33.29	24.22	43.70	1.20	25.94	3.05	8.75
28X-2, 1-3	256.11	44.05	4.65	1.61	9.63	27.27	18.47	25.40	1.27	16.40	3.11	5.18
107-654A-												
6R-4, 137-139	46.17	21.84	2.04	1.09	8.92	34.00	28.11	44.40	1.12	30.63	4.24	3.18
36R-2, 41-42	311.91	6.66	0.80	0.15	3.00	48.14	37.88	58.10	1.44	33.78	1.91	26.94
38R-1, 130-132	330.60	24.41	2.83	0.57	8.79	35.51	24.04	38.50	1.39	27.01	1.98	12.18
38R-2, 44-46	331.24	21.34	2.65	0.57	6.86	37.87	26.11	42.10	1.49	24.11	2.27	13.92
107-655A-												
3H-4, 69-71	17.89	3.27	0.61	0.15	3.59	1.91	1.59	90.20	2.24	82.34	3.90	1.05

From the chloroform extracts, the saturated hydrocarbons, isolated by a thin-layer chromatography technique (Huc et al., 1977), have been analyzed by gas chromatography.

CHARACTERIZATION OF THE ORGANIC MATTER IN THE MESSINIAN SAMPLES

The Messinian deposits of Hole 652A present generally low ($0.5 < \text{TOC} < 1\%$) to extremely low ($\text{TOC} < 0.1\%$) values of Total Organic Carbon, except in the finely laminated black shales encountered around 600 m depth. In these black shales, TOC reaches 13.65% and the petroleum potentials are very high (up to 129 kg HC/t of rock) (Table 1).

The few Messinian black shales of Hole 653B that have been analyzed present moderate contents of organic carbon ($0.5 < \text{TOC} < 2\%$) (Table 1).

The sample of Unit II in Hole 654A is devoid of organic matter ($\text{TOC} = 0.03\%$). The other Messinian samples from the very finely laminated black shales of Unit III, present moderate to fair TOC values (between 0.8% and about 4%), with good petroleum potentials (Table 1).

In a HI vs. OI diagram (Fig. 2), the Messinian sediments are highly scattered. The very organic-rich black shales of Hole 652A coincide with the initial evolution path of the classical Type I (Tissot and Welte, 1978). The other samples are disseminated between the Type II and the Type III trends (Tissot and Welte, 1978), and probably reflect a large variety of sources and/or depositional environments. Such a variety is even observed at the scale of individual units of the Messinian sediments, as the lithologic unit III of Hole 654A: sample 107-654A-38R-2, 44-46 cm, plots at the beginning of Type II path, while 107-654A-38R-1, 126-13 cm, is near the beginning of the Type III path. Between these two samples, 107-654A-38R-1, 130-132 cm, has an intermediate composition, which probably means a mixing of organic matter from different origin.

This picture is confirmed by the plot of kerogens KC in a Van Krevelen diagram (Fig. 3). Samples from Hole 652A appear as the most heterogeneous: one sample is located at the beginning of the Type III trend, which serves as a reference for the organic matter derived from terrestrial plants; two samples (the two samples already noticed for their high petroleum potential) are located in an intermediate position between Type I and Type II trends, which serve as reference for organic matter derived re-

spectively from algal (especially lacustrine) lipids or from organic matter enriched in lipids by microbial activity, and from marine planktonic biomass (Tissot and Welte, 1978).

The samples from the two other sites appear to be mixtures of a hydrogen-rich end-member (Type I or Type II) and an oxygen-rich end-member (Type III). The difference observed between 107-654A-38R-2, 44-46 cm, and 107-654A-38R-1, 130-132 cm, in the (HI, OI) diagram (Fig. 2) disappears in the Van Krevelen diagram (Fig. 3). Nevertheless this difference cannot be explained by a matrix effect, because HI of the corresponding KC are themselves very different from each other (Table 1).

The diversity of organic matter quantities and qualities in the Messinian deposits of ODP Leg 107 reflects a diversity of paleoenvironmental conditions during sedimentation as well as during early diagenesis. This variety has also been observed through nannoplankton study (Müller, this volume): the general evolution in the Tyrrhenian Sea during this epoch is a transition from open marine conditions (Tortonian-lower Messinian) to marine restricted or lacustrine environments (upper Messinian). In such a context, very peculiar situations may develop locally: for instance, Unit III of Hole 654A would have been accumulated under the sea but with possibly high productivity and notable input of terrestrial organic debris (Müller, this volume), while Unit V of Hole 652A would have been accumulated, at least in part, under lacustrine conditions.

CHARACTERIZATION OF THE ORGANIC MATTER IN THE PLIOCENE-PLEISTOCENE SAMPLES

The organic matter present in the discrete sapropelic layers of Pliocene-Pleistocene age, when compared to the Messinian one, gives a totally different picture: in the HI-OI diagram (Fig. 4), as well as in the Van Krevelen diagram (Fig. 5), the samples cluster tightly around an intermediate composition between Type II and Type III. Probably, higher proportions of Type III than of Type II are present in the sediments.

Whatever the way invoked to explain the deposition of sapropels, the organic content of Pliocene-Pleistocene ones reflects a paleoenvironment rather subject to external and relatively terigenous influences, especially when compared to restrictive conditions developed here and there during Messinian.

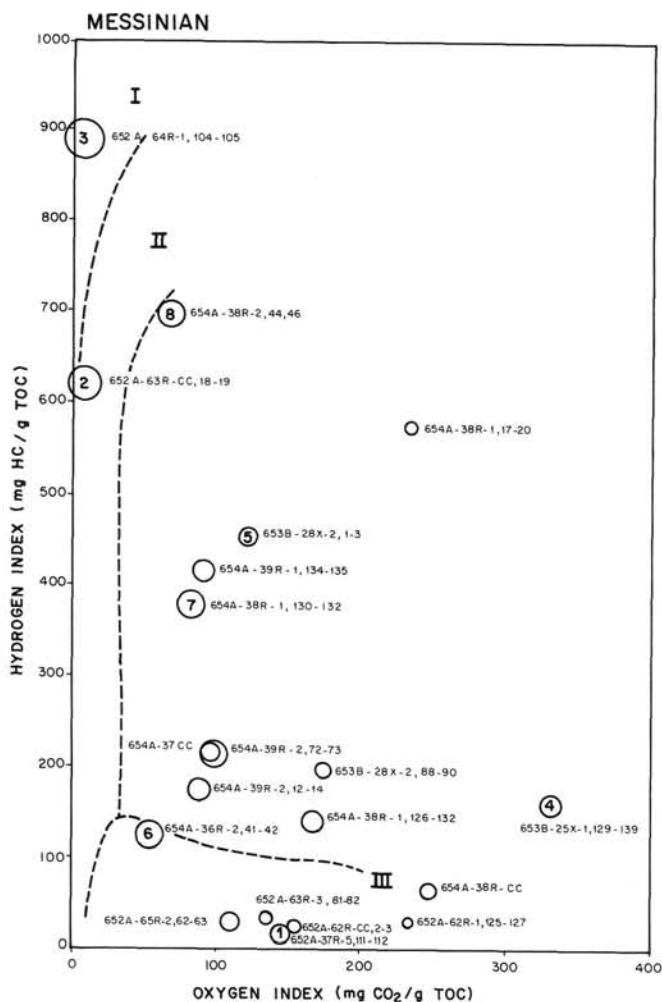


Figure 2. HI vs. OI for Messinian crude rock samples. HI is the Hydrogen Index (S_2/TOC , in mg HC/g TOC). OI is the Oxygen Index (S_2/TOC , in mg CO_2/g TOC). Symbol size is proportional to the TOC value. The numbers in the symbols correspond to the analyzed kerogens (Fig. 3). I, II, and III are the trends defined by Tissot et al. (1974).

DISCUSSION: MATURITY AND NATURE OF THE ORGANIC MATTER

The pyrolysis temperatures T_{max} of most of the samples is less than $426^\circ C$, and consequently the organic matter as a whole may be considered as immature. Nevertheless, several points must be underlined and discussed.

1. A systematic and significant difference does exist between T_{max} of the samples which come from Hole 654A ($\sim 400^\circ C$) and T_{max} of the samples which come from other sites ($\sim 420^\circ C$).

2. There is no observable T_{max} increase as a function of depth. In Hole 652A for instance, T_{max} values for the less buried samples ($420^\circ C$, $422^\circ C$, at ~ 69 m) and for the most buried one ($426^\circ C$, at ~ 626 m) are about the same; and very young sediments, such as 107-655A-2H-4, 65-66 cm, at only 5 mbsf, present a comparable T_{max} ($421^\circ C$).

3. The two black shales of Hole 652A which have a very high petroleum potential (107-652A-63R-CC, 18-19 cm, and 107-652A-64R-1, 104-105 cm) present higher T_{max} values than all other samples ($435^\circ C$ and $437^\circ C$, respectively).

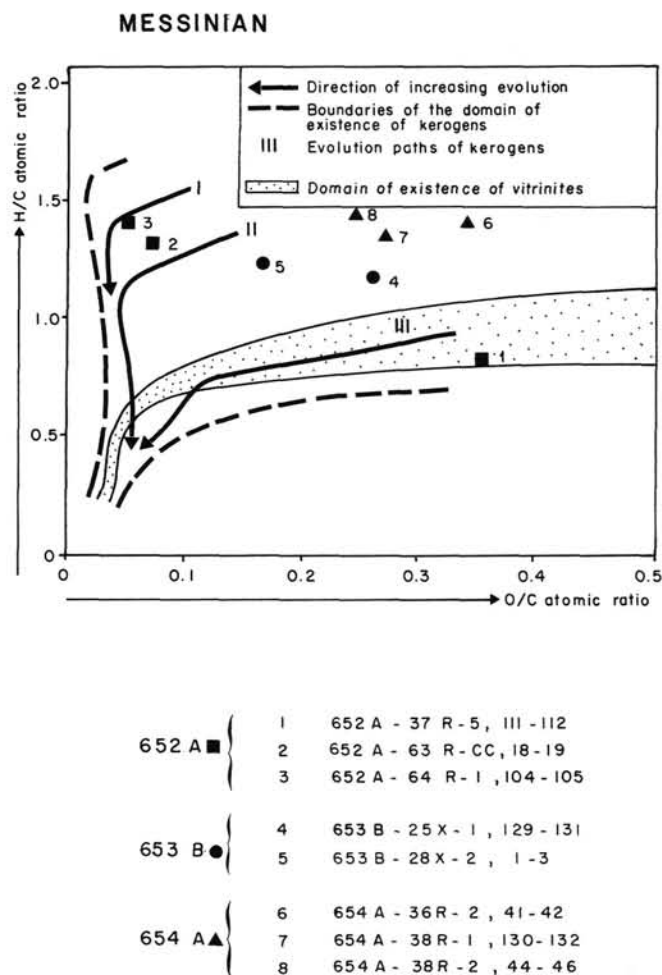


Figure 3. Atomic H/C vs. O/C for Messinian extracted kerogens.

On the other hand, it has been verified on the pyrolysis diagrams that the S_2 peaks are sufficiently well defined to provide a meaningful T_{max} . The lack of a systematic and important gap between T_{max} of the crude rocks and T_{max} of the chloroform extracted rocks, or T_{max} of the kerogens (Table 1), ensures that these values reflect an intrinsic state of the organic matter. As a consequence, the differences noticed above may be interpreted only in two ways: variations in the nature of the organic content, or differences in the thermal alteration reached by this organic content. As a matter of fact, a very marked difference does exist between heat flows at Site 654 and at the other sites (Kastens, Mascle, et al., 1987) and it seems likely that the lower T_{max} of this site can be explained by its relatively moderate thermal regime. Nevertheless the arguments which favor the first interpretation (variations in the nature of the organic content) are stronger according to our present analytical investigation:

1. No correlation of T_{max} vs. depth;

2. Highest T_{max} observed for two samples which are characterized by a specific composition in the HI-OI diagram as well as in the Van Krevelen diagram (Figs. 2 and 3), and also by peculiar chromatographic distributions of the saturated hydrocarbon fraction from the chloroform extracts (Fig. 6).

If this interpretation is retained, no clear explanation for the particular case of Hole 654A can be given for the moment, be-

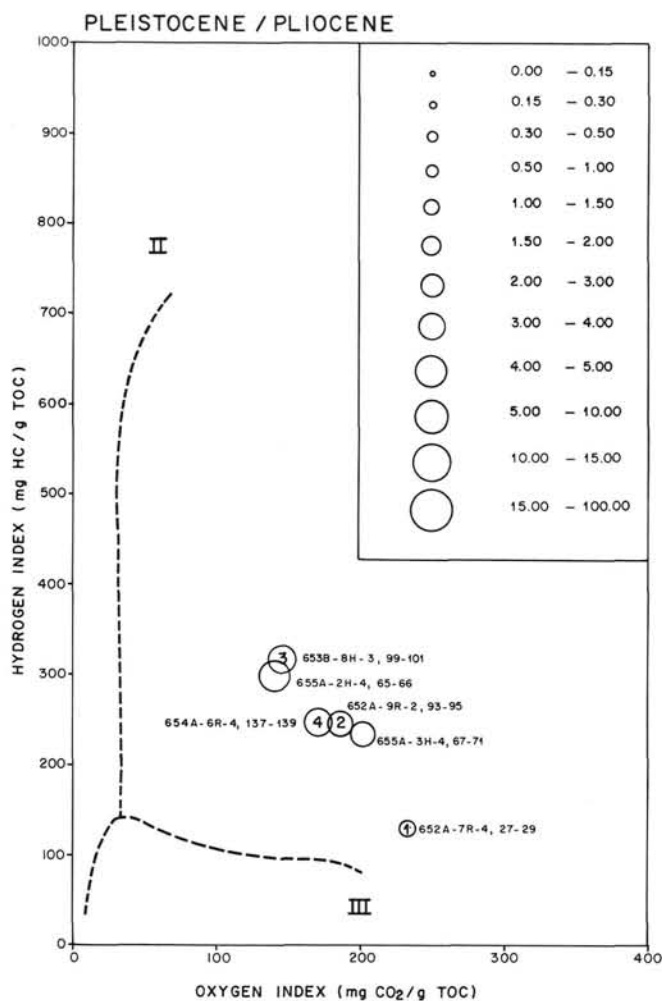


Figure 4. HI vs. OI for Pliocene-Pleistocene whole rock samples.

cause there is no observable evidence, in HI-OI or Van Krevelen diagrams, of a peculiar nature of the organic matter.

CONCLUSION

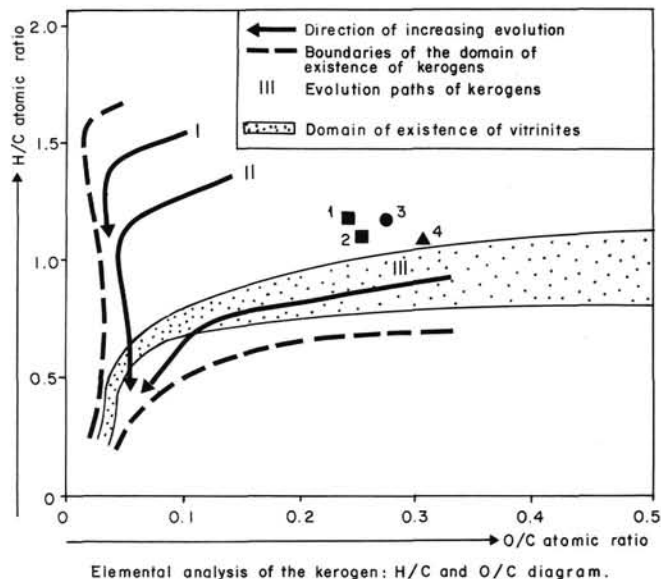
The Messinian black shales from Holes 652A, 653B, 654A, and 655B of the ODP Leg 107 (Tyrrhenian Sea) are characterized by a large variety of organic compositions, observed through the Rock-Eval pyrolysis of rock samples and through the elemental analysis of kerogens. This variety probably reflects a great diversity of depositional and diagenetic paleoenvironments, changing from marine to lacustrine conditions with a more or less abundant terrestrial contribution.

In contrast, the Pliocene-Pleistocene sapropels present a rather homogeneous organic content, highly influenced by terrigenous organic matter, but with a systematic participation of marine algal organic matter. This homogeneity probably means a periodic reinstallation of special marine conditions favorable to the preservation of the sedimented organic matter.

REFERENCES

Borsetti, A. M., Carloni, G. C., Cato, F., Ceretti, E., Cremonini, G., Elmi, C. and Ricci Lucchi, F., 1975. Paleogeografia del Messiniano nei bacini Periadriatici dell'Italia settentrionale e centrale. *G. Geol.*, 40:21-72.

PLEISTOCENE / PLIOCENE



Elemental analysis of the kerogen: H/C and O/C diagram.

- 652 A ■ 1 652 A - 7R - 4, 27 - 29
- 652 A ■ 2 652 A - 9R - 2, 93 - 95
- 653 B ● 3 653 B - 84 - 3, 99 - 101
- 654 A ▲ 4 654 A - 6R - 4, 137 - 139

Figure 5. Atomic H/C vs. O/C for Pliocene-Pleistocene extracted kerogens.

Carloni, G. C., Cato, F., Ceretti, E., Cremonini, G., Elmi, C., and Ricci Lucchi, F., (1974. Messialano Padona Adriatico: descrizione di trenta sezioni rappresentative. *Bol. Ser. Geol. It.*, 95:89-114.

Cita, M. B., 1982. The Messinian salinity crisis in the Mediterranean: a review. In Berckhemer, H., and Hsü, K. J. (Eds.). *Alpine Mediterranean Geodynamics: Geodynamic Ser.*, 7:113-140.

Deroo, G., Herbin, J. P., and Roucache, J., 1978. Organic geochemistry of some Neogene cores from sites 374, 375, 377 and 378: Leg 42 A, Eastern Mediterranean Sea. In Hsü, K. J., Montadert, L., et al., *Init. Repts., DSDP 42 (Pt. 2):* Washington (U.S. Govt. Printing Office), 465-472.

Drooger, C. W., 1973. *Messinian events In the Mediterranean*, North Holland Publishing Company.

Durand, B., and Monin, J. C., 1980. Elemental analysis of kerogens. In Durand, B., (Ed.) *Kerogen: Technip*, 113-142.

Durand, B., and Nicaise, G., 1980. Procedures for kerogen isolation. In Durand, B., (Ed.) *Kerogen: Technip*, 35-54.

Espitalie, J., Marquis, F., and Barsony, I., 1984. Geochemical logging. In Voorhees, K. J. (Ed.), *Analytical Pyrolysis: Butterworth*, 276-304.

Espitalie, J., Deroo, G., and Marquis, F., 1985a. *La pyrolyse ROCK-EVAL et ses applications*. Rev. Inst. Fr. du Pétrole, 40:563-579.

_____, 1985b. *La pyrolyse ROCK-EVAL et ses applications*. Rev. Inst. Fr. du Pétrole, 40:755-784.

_____, 1986. *La pyrolyse ROCK-EVAL et ses applications*. Rev. Inst. Fr. du Pétrole, 41:73-89.

Huc, A. Y., Roucache, J., Bernon, M., Caillet, G., and Da Silva, M., 1977. *Application de la chromatographie sur couche mince à l'étude quantitative et qualitative des extraits de roche et des huiles*. Rev. Inst. Fr. Pétrole, 31:67-98.

Kastens, K., Mascle, J., et al., 1988. ODP Leg 107 in the Tyrrhenian Sea: Insights into passive margin and back-arc basin evolution. *Geol. Soc. Am. Bull.*, 100:1140-1156.

Kidd, R. B., Cita, M. B., and Ryan, W.B.F., 1978. Stratigraphy of Eastern Mediterranean sapropel sequences recovered during D.S.D.P. Leg 42A and their paleoenvironmental significance. In Hsü, K. J., Montadert, L., et al., *Init. Repts., DSDP*, 42 (Pt. 1): Washington (U.S. Govt. Printing Office), 421-443.

Steinmetz, L., Ferruci, F., Hirn, A., Morelli, C., and Nicolich, R., 1983. A 550 km long Moho traverse in the Tyrrhenian Sea from O.B.S. recorded P_n waves. *Geophys. Res. Lett.*, 10:428-431.

Tissot, B. P., and Welte, D. H., 1978. *Petroleum formation and occurrence*. Springer-Verlag, 1-538.

Date of initial receipt: 18 November 1987

Date of acceptance: 2 December 1988

Ms 107B-115

GAS CHROMATOGRAPHY OF SATURATED HYDROCARBONS

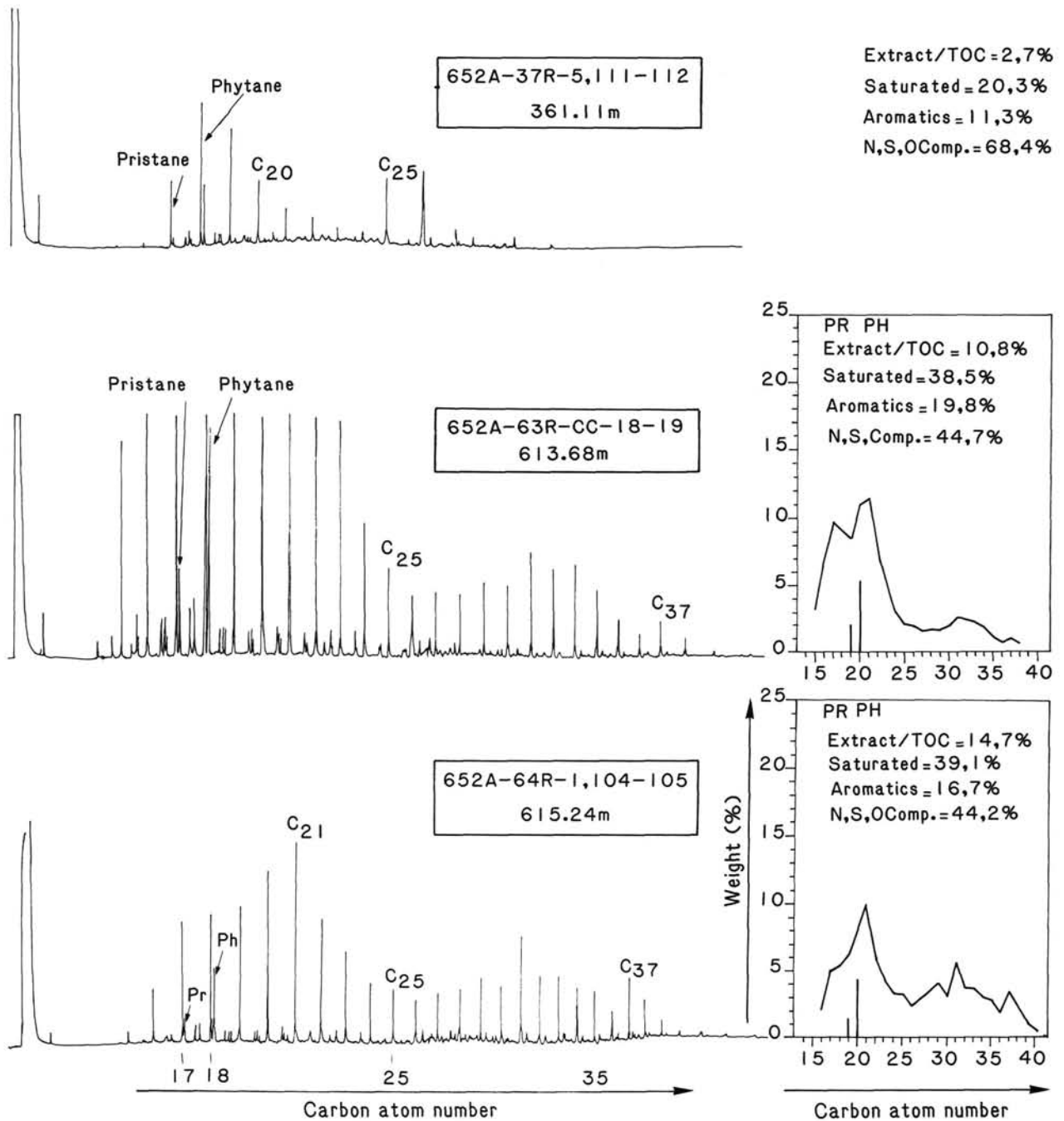


Figure 6. Gas chromatography of the saturated hydrocarbons. In most of the samples (e.g., 107-652A-37R-5, 111-112 cm), Extract/TOC is low (few %), the N, S, O, and heavy molecular weight compounds are dominant. In the two Messinian samples of Hole 652A which have a very high petroleum potential (107-652A-63R-CC, 18-19 cm, and 107-652A-64R-1, 104-105 cm), Extract/TOC is much more elevated (up to ~15%), together with saturates and aromatics fractions, and the gas chromatography of the saturated hydrocarbons give a very extended and well-developed picture, where a moderate odd-carbon-numbered preference and a low pristane/phytane ratio may be noticed. The faint odd-carbon-numbered predominance in the *n*-alkanes of high molecular weight (*n*-C₂₅ to *n*-C₃₇) could be a very discrete fingerprint of continental organic matter: it is well known in oil shales like Green River shale, which serve as a reference series for the Type I kerogen definition (Tissot and Welte, 1978).